Modeling and Simulation of a UV Water Treatment System Fed by a GPV Source Using the Bond Graph Approach

Riahi Said
UR-LAPER, Faculty of Sciences of Tunis
University of Tunis El Manar
Tunis, Tunisia
riahi.said@fst.utm.tn

Naoufel Zitouni
UR-LAPER, Faculty of Sciences of Tunis
University of Tunis El Manar
Tunis, Tunisia
naoufel_zitouni@yahoo.fr

Viorel Minzu
Control and Electrical Engineering Department
Dunarea de Jos University
Galati, Romania
Viorel.Minzu@ugal.ro

Abdelkader Mami
UR-LAPER, Faculty of Sciences of Tunis
University of Tunis El Manar
Tunis, Tunisia
abdelkader.mami@fst.utm

Received: 15 February 2022 | Revised: 4 March 2022 | Accepted: 5 March 2022

Abstract-This work presents a simulation model for a UV water treatment system, powered by a photovoltaic generator, which relates the current consumed by the lamp to the UV flux and water quality. The overall system also includes electronic converters, electronic ballast (RLC resonant circuit), a UV lamp (UV irradiation source), and a centrifugal pump. To optimize the power transfer from the PV generator to the ballast and the UV lamp, a Maximum Power Point Tracking (MPPT) device is used. The overall water treatment system presents a complex model due to its hybrid components. The bond graph tool with a multidisciplinary vocation allows precisely, by its graphic nature, using a unified language, to explicitly display the nature of the power exchanges in the system and facilitate its control. This tool is a solution for non-linear systems that guarantees and facilitates their modeling without difficulties.

Keywords-bondbraph; UV water treatment system; complex model; photovoltaic generator; centrifugal pump; simulation

I. INTRODUCTION

Several water resources may be untreated and therefore they can be factors of transmission of diseases. The reuse of wastewater after an adequate treatment by UV radiation, presents a very good solution to solve the problems related to water pollution and constitutes a potential water resource. The majority of the existing UV disinfection systems use low pressure mercury arc lamps as a source of UV radiation that generates short waves in the region of 253,7nm [1-3]. The discharge lamp is placed in a reactor and is surrounded by a quartz tube immersed in a chamber in which the fluid is circulated. It is powered by an energy source such as a photovoltaic generator via an electronic ballast composed of an inverter, a transformer and a resonant circuit (RLC) [4, 5]. A centrifugal motor pump as shown in Figure 1 ensures the circulation of water between the two tanks. The physico-chemical parameters (pH, temperature, etc.), the applied UV dose, the exposure time, as well as the number and type of microorganisms, are factors that can influence the final water quality. Many studies have been developed to improve water treatment systems despite their complexity, especially of the UV lamp model [6-8].

The aim of this study was to build a simulation model for all the components of the complex UV water treatment system shown in Figure 2. The bond graph approach is a modeling tool that facilitates the links between the different physical domains (mechanical, hydraulic, electrical) that represent the overall system. A photovoltaic (PV) generator model is presented in the first section along with the MPPT control in order to adapt the PV source and the load with a simulation result.

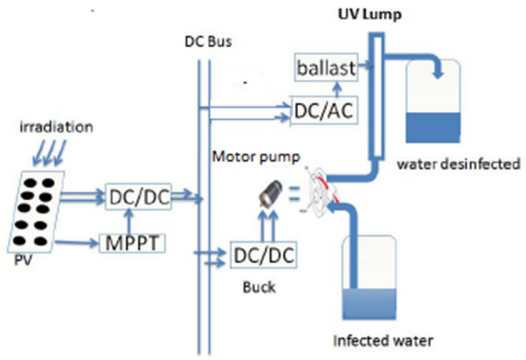

Fig. 1. Structure of the overall UV water treatment system powered by a PV panel.

Corresponding author: Abdelkader Mami

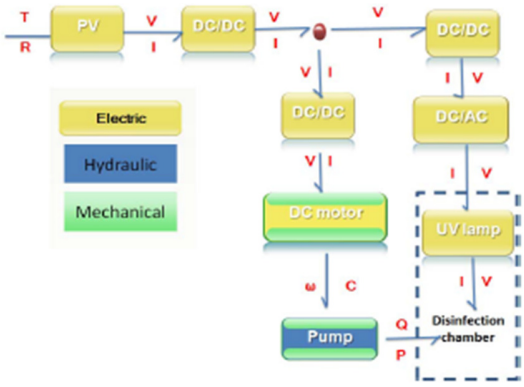

Fig. 2. Representation of the energy exchanges in the system with different physical fields.

II. MODELING OF THE PV SOURCE BY THE BOND GRAPH APPROACH

A. The PV Generator Model

In order to power UV water disinfection systems with solar energy in a simple and inexhaustible way, we need to use PV generators. PV panels are characterized by the non-linearity of their output which is influenced by environmental factors (temperature and irradiation). The PV model used has two resistors in series and in shunt as shown in the equivalent electrical diagram in Figure 3.

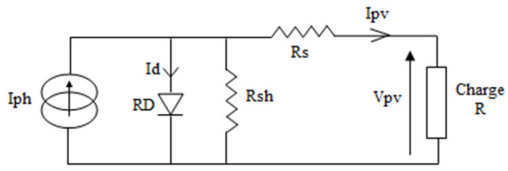

Fig. 3. Equivalent electrical circuit of a single diode PV generator.

The simplified equation of the PV current is:

$$I_{pv} = I_{ph} - I_0\left[\exp\left(\frac{q\times(V+I\times R_s)}{n\times K\times N_s\times T}\right)-1\right]-I_{sh} \quad (1)$$

where I_{pv} is the the output current, I_0 the diode inverse saturation current, and R_s the series resistor. K is the Boltzmann's constant, q is the electronic charge, n is the ideal diode factor ($1<n<2$) for a unique junction, and T is the functioning temperature. The current through the shunt resistor is given by:

$$I_{sh} = (V_{pv} + I_{pv}\times R_s)/R_{sh} \quad (2)$$

The photocurrent generated by the cell depends on the ambient temperature (T) and the solar irradiation (G) and is represented by:

$$I_{ph} = I_{sc} + K_I\cdot(T-298)\cdot\mathbf{G}/1000 \quad (3)$$

B. Bond Graph Model of the Photovoltaic Generator

A simplified model that does not take into account the losses was adopted. This model is called mono-diode coupled to a starting capacitor that is placed in parallel with the photovoltaic generator. The added capacitance represents the capacitance of the PN junction and it depends on the voltage Vd.

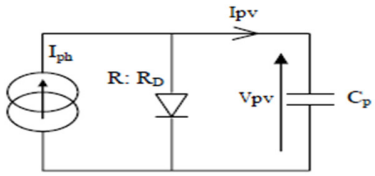

Fig. 4. Electrical diagram of the PV generator with starting capacity.

The bond graph model for the equivalent circuit is presented in Figure 5. It contains an element of capacitance, and the element noted as R_D is the resistance of the diode. It contains the non-linear characteristic. This allowed us to replace the generator by a modulated flux source S_f which plays the role of the modulating signal representing the photovoltaic current I_{ph}. This model was simulated by the software 20-sim [6, 9-11].

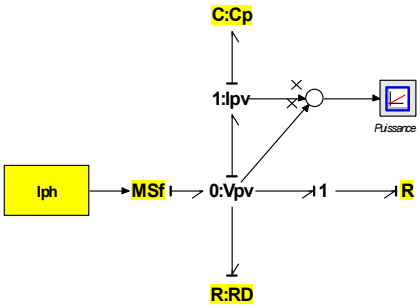

Fig. 5. Bond graph of the PV model.

To simulate the characteristics of the photovoltaic panel I=f(V) and P=f(V) [18-19], we use the BG model shown in Figure 5. In this simulation, the receiver is an initially discharged capacitor. The simulation results are represented in Figure 6.

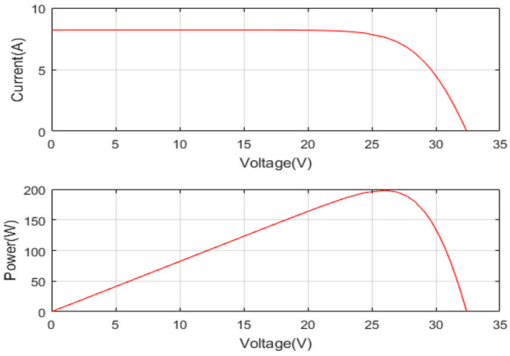

Fig. 6. Simulation of the characteristic curves of the PV system.

III. CONVERTERS USED

Static converters are mainly made up of semiconductor components that work in switching mode (thyristors, power

transistors, etc.). In our UV system, the converters are placed as follows: a first chopper booster is inserted between the UV lamp and the PV generator, a second chopper devolver is inserted between the motor pump and the PV panel, and a single-phase inverter generates a square voltage.

A. Dynamic Boost Converter

As the name suggests, this type of static converter amplifies the output voltage relative to the input voltage. In electronic structure, a boost chopper generally has a switch controlled on opening and closing (transistor, IGBT) and a diode [14, 15].

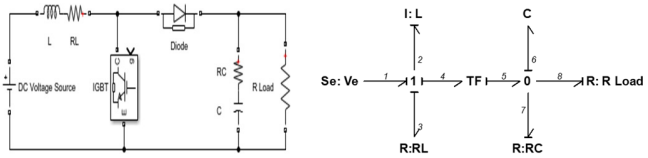

(a) (b)

Fig. 7. Boost converter: (a) equivalent model, (b) its bond graph model.

B. Dynamic Buck Converter

The static converter (DC/DC) used, is most frequently used as a devolving converter, its basic schematic is that of Figure 8. A buck converter converts a DC voltage into another DC voltage of lower value [11, 16-18].

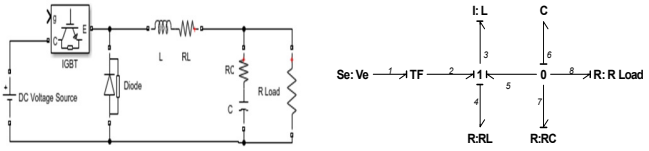

(a) (b)

Fig. 8. Buck converter: (a) equivalent model, (b) its bond graph model.

C. Single Inverter

The resonant circuit (electronic ballast) requires a square voltage, which is obtained with an inverter, which is a static converter that converts electrical energy from DC to AC. It allows obtaining an alternating voltage adjustable in frequency and in RMS value, thus using an appropriate control sequence.

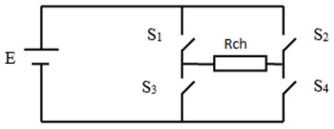

Fig. 9. Equivalent electrical diagram of a single-phase inverter.

D. Bond Graph MPPT: Perturbation and Observation Algorithm

The Perturbation and Observation (P&O) method is a widely used approach in MPPT research, because it is a simple iterative method. It can track the Maximum Power Point (MPP) even during sudden changes in irradiance and temperature [2, 9, 11, 17, 20]. Using the P&O algorithm, a link graph MPPT model was developed (Figures 11-12).

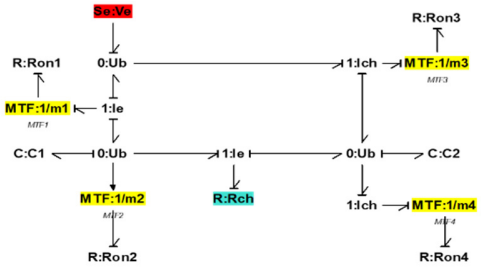

Fig. 10. Bond graph model of a single inverter.

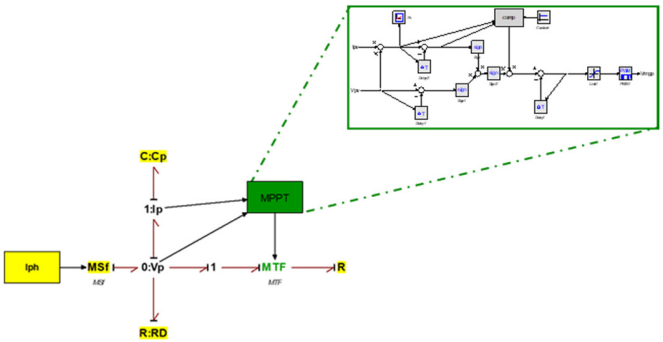

Fig. 11. Adaptation model of an MPPT converter with a PV panel by bond graph.

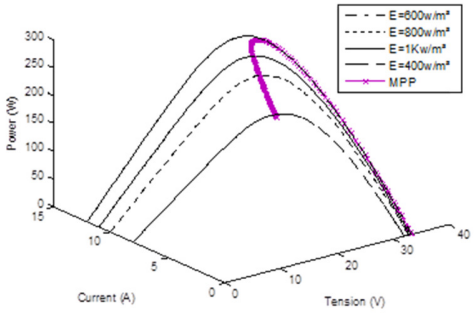

Fig. 12. Simulation of the P&O control algorithm for different illuminations.

IV. BOND GRAPH MODELING OF THE ELECTRONIC BALLAST AND THE UV LAMP

The electronic power supply (electronic ballast) of a UV lamp can be broken down into three parts: The DC/AC converter, which is described above, the transformer, and the resonant circuit.

A. The Resonant Circuit (Electronic Ballast)

A discharge lamp needs sufficient voltage to light up. This lamp uses an electronic ballast capable of creating a high frequency voltage and an increase in the voltage value on the UV lamp for a short time. This overvoltage is obtained by a resonant circuit (RLC). The voltage delivered by the DC/AC converter, feeds a transformer to a resonant system formed by a resistor Rr in series with an inductance Lr and two capacitors Cr1 and Cr2 (Figure 13) The receiver is a discharge lamp (UV) which is compared to an infinite impedance before start-up and to a low value impedance after start-up [4, 5]. The corresponding bong-raph model is shown in Figure 14.

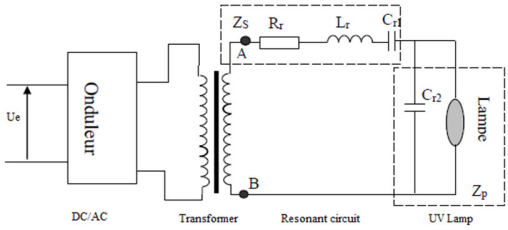

Fig. 13. Equivalent electrical diagram of a UV lamp power supply.

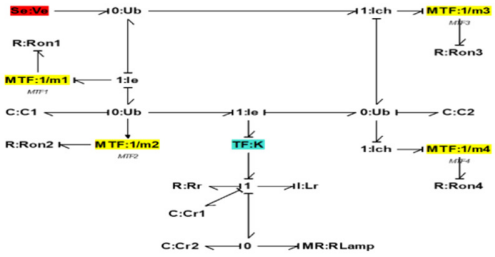

Fig. 14. Bond-graph model of the irradiation system.

B. The UV lamp

The UV water treatment system consists of a high pressure lamp placed vertically in a quartz sheath to be thermally isolated from the water. This lamp is assembled in a closed reactor. The water circulates in thin layers in the vicinity of the lamp because the UV rays are rapidly absorbed by the water. The disinfection efficiency obtained varies between 90% and 99.99%, depending on the duration of exposure of the water to radiation and the characteristics of the water to be treated. Certain electrical circuits generated by electronic ballasts are required to start the discharge lamp, to regulate the lamp cycle, and to control the electrical current.

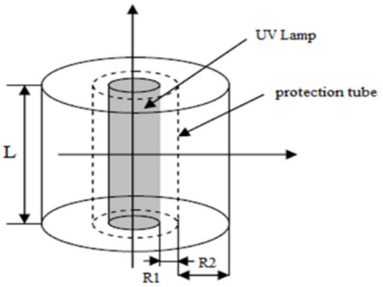

Fig. 15. Schema of the UV reactor.

There are several models based on the current-voltage characteristics of the high-frequency discharge when trying to find a function that describes the relationship between current, voltage, and power consumed by the lamp. The UV lamp has a complicated model, it is in conjunction with an electronic ballast as described in (1):

$$U_e(t) = R_{Ballast} i(t) + L_{Ballast} \frac{di(t)}{dt} + U_{Lamp}(t) \quad (1)$$

The universal lamp model is defined by:

$$U_{Lamp}(t) = \frac{I_{Lamp}(t)}{G(t)} \quad (2)$$

The literature describes the conductance of a discharge lamp by a first-order differential equation, named G-model [1, 21, 22], which is presented as follows:

$$\frac{dG}{dt} = a_2 i^2 - \sum b_n G^n \quad (3)$$

where the coefficients α_2 and b_n can be determined experimentally from the voltage-current characteristics or by physical evaluation. The physical evaluation is possible when n is equal to 2 or 3. In this case, the coefficients have a physical meaning:

$$\frac{dG}{dt} = a_2 i^2 - b_2 G^2(t) - b_1 G(t) \quad (4)$$

The determination of the parameters α_2, b_1, and b_2 is done using an identification approach. According to (4), we developed the bond graph model of the UV lamp. Figure 16 exhibits the established model of the UV lamp.

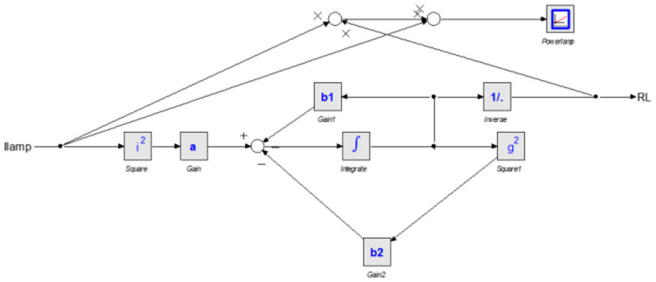

Fig. 16. Bond graph model of the UV lamp.

V. BOND-GRAPH MODELING OF THE HYDRAULIC SYSTEM

The hydraulic system is a very important part of the water treatment system. It consists of a direct current motor connected to a centrifugal pump.

A. Modeling of the DC motor

The water treatment system has a motor pump to draw contaminated water from the inlet tank as shown in Figure 17. The motor pump subsystem must be able to control the flow rate of the contaminated water, which will determine the UV exposure time. Equation (5) expresses the latter:

$$t_{\text{exposure}} = V / Q \quad (5)$$

The values V and Q are the volume of the reactor and the flow rate of water respectively. The variation of Q determines the possibility to control the exposure time and consequently the UV dose received by the water [6, 10, 11, 23].

The dynamics of the engine [5, 10], are described by:

$$U_a = R_a I_a + L_a \frac{dI_a}{dt} + K_b w \quad (6)$$

$$C_m = J_m \frac{dw}{dt} + Fw + C_r \quad (7)$$

The DC motor is modeled in bond-graph by inertial elements I:La and resistive elements R:ra, representing respectively the inductance and the resistance of the armature. A gyrator models the transfer of energy from the electrical part to the mechanical part K_b ($E_a = K_b w$). The mechanical losses are modeled in bond graph by an inductive element I:J and a resistive element R:f which indicate respectively the coefficients of inertia and viscous friction of the DC machine. The DC motor drives a centrifugal pump characterized by a rotor shaft Γ proportional to the square of speed w ($\Gamma = K_T w^2$). Figure 18 presents the bond graph model of a DC motor.

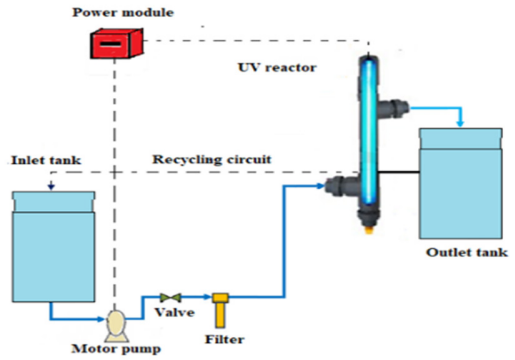

Fig. 17. Schematic representation of the location of a DC motor in the UV water treatment system.

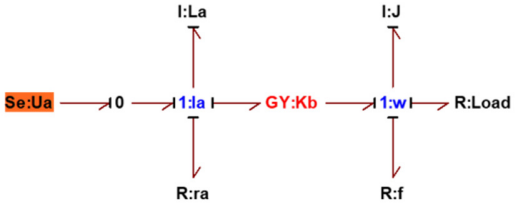

Fig. 18. Bond graph model of a DC motor.

B. Modeling of the Centrifugal Pump

The water disinfection operation consists of water circulating through a UV reactor. Once the pump is running, the rotation of the impeller produces pressure and a speed that determines the flow of the fluid in the hydraulic system [5, 10, 14]. The theoretical head H_e developed by a centrifugal pump is given by:

$$H_e = \frac{w^2 r_2^2}{2g} \quad (8)$$

The pressure developed by the wheel is directly proportional to the angular velocity w. The shaft speed is proportional to the flow rate Q. The developed pressure and the transmitted torque have the following expressions:

$$P_e = \rho g H_e = \frac{\rho r_2^2 w^2}{2} \quad (9)$$

$$T_e = \frac{\rho r_2^2 w}{2} Q \quad (10)$$

The relationship between the pressure supplied by the pump and the rotation speed, can be modeled in bond-graph by a modulated gyrator element, MGY. The latter transforms the mechanical flow (speed) into hydraulic force (pressure). The pressure losses in the pump are due to the friction between the liquid threads and against the walls of the machine:

$$T_{fp} = f_{mp} w \quad (11)$$

This friction is modeled in bond-graph by a resistive element R:f_{mp} and the moment of inertia of the rotating parts of the pump has the following expression:

$$T_{ip} = J_{pt} \frac{dw}{dt} \quad (12)$$

This moment of inertia is modeled in bond-graph by an inertial element I:J_{pt}.The pressure losses in the hydraulic circuit are due to the friction of the flow lines against the walls of the machine. They are modeled by a resistive element R:$f_{\xi d}$. The height difference between the two tanks is modeled by a negative force source:

$$Se = -\delta g H_e \quad (13)$$

The associated bond graph model of the centrifugal pump is shown in Figure 20.

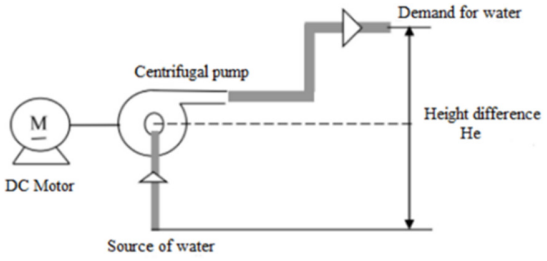

Fig. 19. Synoptic diagram of a centrifugal pump.

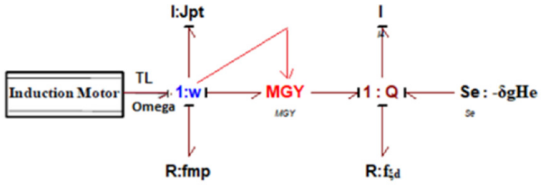

Fig. 20. Bond graph model of the centrifugal pump.

For a stationary regime (constant speed), the characteristic of the theoretical head of a pure centrifugal pump in vacuum (isolated from the hydraulic network) can be seen in Figure 21.

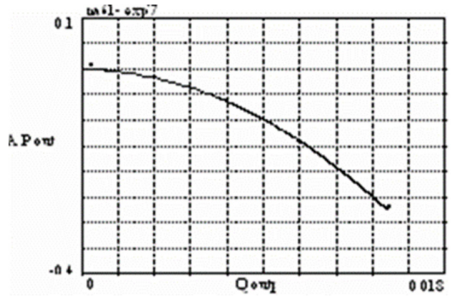

Fig. 21. H_e (Q) simulation characteristic of a centrifugal pump.

VI. GLOBAL MODEL OF A WATER TREATMENT SYSTEM BY BOND GRAPH

After having modeled the different elements of the water treatment system and simulated the obtained models, we can deduce the global model (BG) by combining the different models obtained, which is presented in Figure 22.

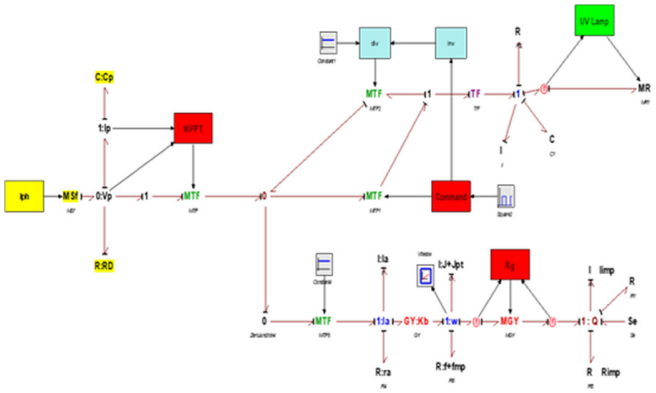

Fig. 22. Global model of the global UV water treatment unit

VII. SIMULATION RESULTS

The UV water treatment system consists of a closed cylindrical stainless steel reactor with an annular cross-section, 70cm in length, 6cm in internal diameter and 2L of useful volume. It is equipped with a single low-pressure mercury discharge lamp with the following characteristics: power 70W, nominal current 0.65A, length 400mm, diameter 15mm, placed in the axis of the irradiation room and protected by a clean quartz sleeve. The lamp is powered by an electronic ballast consisting of a single-phase inverter with transistors producing 25-100kHz at its output and a resonant circuit to realize the ignition of the lamp. The disinfection system is also equipped with a motor pump for the suction of contaminated water, a pump to draw contaminated water from the inlet tank, a flow control valve to obtain different flow rates, and a filter to improve the transmittance of the contaminated water. The treated water in this system could be recycled through a recirculation circuit that could allow multiple passes through the irradiation chamber.

According to the global model simulation, we obtained the following results: Figure 23 shows the output voltage of the single-phase inverter, which converts DC voltage to AC voltage to power the ballast and UV lamp, as they require AC voltage. The voltage and current curves of the UV lamp (discharge lamp) are shown in Figures 24 and 25 with the following values: the voltage is approximately 150V and the current 1.42A. The parameters of the UV lamp and the electronic ballast are: a_2=93.33, b_2=582036.5, b_1=994.7, R=0.9Ω, C=2.8µF, L=0.16mA. Figure 26 describes the evolution of the conductivity G of the UV lamp.

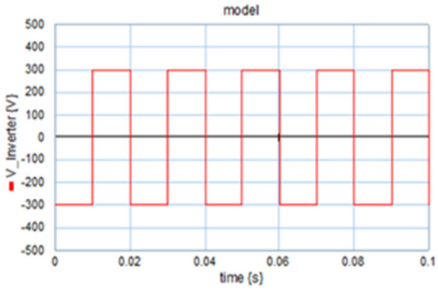

Fig. 23. Simulation of the output voltage of the inverter.

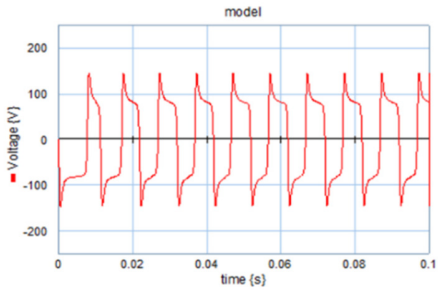

Fig. 24. The voltage of the UV lamp.

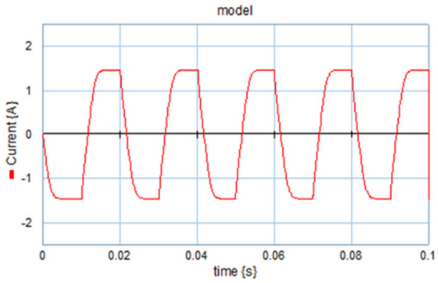

Fig. 25. The current of the UV lamp.

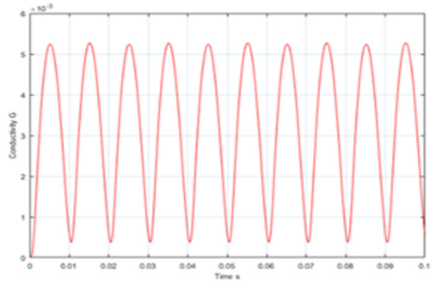

Fig. 26. The conductivity of the UV lamp.

Due to the negative impedance of discharge lamps and the complexity of the analysis, it is difficult to obtain models for the discharge lamps due to their negative impedance and the

complexity of the physical phenomena that occur inside the discharge tube. Discharge lamps can be operated at different frequencies with electronic ballasts. These different operating conditions can affect the behavior of the lamp. Generally, the non-linear *I-V* characteristic of the discharge lamps changes with frequency. Figure 27 represents the evolution of the non-linear obtained *I-V* characteristic after these simulations.

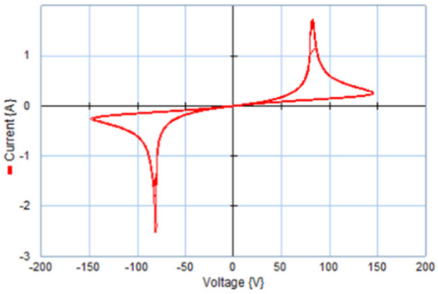

Fig. 27. *I-V* characteristic curve of the UV lamp.

The simulation of the continuous motor pump was performed using the buck converter. The motor voltage *Ua* is 24V. Figure 28 shows the evolution of the induced current, the motor torque, the rotation speed and the water flow. One can see a normal evolution of the four parameters.

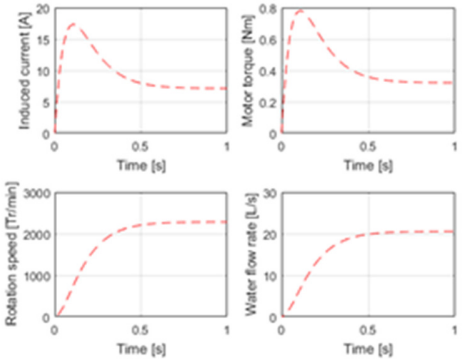

Fig. 28. Evolution of the motor pump's parameters.

VIII. Conclusion

This paper proposes link graph models for each subsystem of a UV water treatment unit. The different elements were connected to produce a dynamic model, which was used as the basis for building the simulation model. Using the 20-Sim software, a general simulation model was proposed. The series of simulations performed proved that the models were realistic and produced useful data. The link graph approach facilitates the connections between the different components of the overall model given the complexity of this unit. Future work could use this global model to determine the optimal parameters for all subsystems under given circumstances. The performance index could be the quality of water disinfection.

References

[1] M. Tlili, "Conductivity Polynomial Model Parameters identification based on Particle Swarm Optimization," *Journal of Control Engineering and Applied Informatics*, vol. 15, no. 4, pp. 58–65, Dec. 2013.

[2] B. Mounaouer and H. Abdennaceur, "Disinfection of Water by UV Irradiation-Modeling and Improvement," *Current Biotechnology*, vol. 1, no. 3, pp. 199–206, 2012, http://doi.org/10.2174/2211550111201030199.

[3] A. A. Paidalwar and I. P. Khedikar, "Overview of Water Disinfection by UV Technology -A Review," *International Journal of Science Technology & Engineering*, vol. 2, no. 9, pp. 213–219, Mar. 2016, https://doi.org/10.13140/RG.2.2.30976.25608.

[4] M. Ben Said, M. Ben Mustapha, and A. Hassen, "The impact of power supply frequency of a low pressure UV lamp on bacterial viability and activities," *Desalination and Water Treatment*, vol. 53, no. 4, pp. 1075–1081, Jan. 2015, https://doi.org/10.1080/19443994.2013.860627.

[5] N. Zitouni, R. Andoulsi, A. Sellami, A. Mami, and A. Hassen, "A new Bond Graph Model of a Water Disinfection System Based on UV Lamp Feed by Photovoltaic Source: Simulation and Experimental Results," *Journal of Automation & Systems Engineering*, vol. 5, no. 2, pp. 79–95, 2011.

[6] V. Minzu, S. Riahi, and E. Rusu, "Optimal Control of an Ultraviolet Water Disinfection System," *Applied Sciences*, vol. 11, no. 6, Jan. 2021, Art. no. 2638, https://doi.org/10.3390/app11062638.

[7] S. Sharma and A. Bhattacharya, "Drinking water contamination and treatment techniques," *Applied Water Science*, vol. 7, no. 3, pp. 1043–1067, Jun. 2017, https://doi.org/10.1007/s13201-016-0455-7.

[8] M. C. Collivignarelli, A. Abbà, I. Benigna, S. Sorlini, and V. Torretta, "Overview of the Main Disinfection Processes for Wastewater and Drinking Water Treatment Plants," *Sustainability*, vol. 10, no. 1, Jan. 2018, Art. no. 86, https://doi.org/10.3390/su10010086.

[9] N. Zitouni, B. Khiari, R. Andoulsi, A. Sellami, A. Mami, and A. Hassen, "Modelling and non linear control of a photovoltaic system with storage batteries: A bond graph approach," *International Journal of Computer Science and Network Security*, vol. 11, no. 6, pp. 105–114, Jun. 2011.

[10] M. Turki, J. Belhadj, and X. Roboam, "Bond Graph modelling and analysis of an autonomous Reverse Osmosis desalination process fed by a hybrid system (photovoltaic-wind)," presented at the Electrimacs 2008, the 9th International Conference on Modeling and Simulation of Electric Machines, Converters and Systems, Quebec, Canada, Jan. 2008.

[11] R. Andoulsi, A. Mami, G. Dauphin-Tanguy, and M. Annabi, "Modelling and simulation by bond graph technique of a DC motor fed from a photovoltaic source via MPPT boost converter," in *Conference of Particle Accelerator (CSSC'99)*, New York, NY, USA, 1987, pp. 4181–4187.

[12] X. H. Nguyen and M. P. Nguyen, "Mathematical modeling of photovoltaic cell/module/arrays with tags in Matlab/Simulink," *Environmental Systems Research*, vol. 4, no. 1, Dec. 2015, Art. no. 24, https://doi.org/10.1186/s40068-015-0047-9.

[13] J. Hahm, J. Baek, H. Kang, H. Lee, and M. Park, "Matlab-Based Modeling and Simulations to Study the Performance of Different MPPT Techniques Used for Photovoltaic Systems under Partially Shaded Conditions," *International Journal of Photoenergy*, vol. 2015, Jan. 2015, Art. no. e979267, https://doi.org/10.1155/2015/979267.

[14] N. E. Benchouia, H. A. Elias, L. Khochemane, and B. Mahmah, "Bond graph modeling approach development for fuel cell PEMFC systems," *International Journal of Hydrogen Energy*, vol. 39, no. 27, pp. 15224–15231, Sep. 2014, https://doi.org/10.1016/j.ijhydene.2014.05.034.

[15] Z. R. Labidi, H. Schulte, and A. Mami, "A Systematic Controller Design for a Photovoltaic Generator with Boost Converter Using Integral State Feedback Control," *Engineering, Technology & Applied Science Research*, vol. 9, no. 2, pp. 4030–4036, Apr. 2019, https://doi.org/10.48084/etasr.2687.

[16] Z. R. Labidi, H. Schulte, and A. Mami, "A Model-Based Approach of DC-DC Converters Dedicated to Controller Design Applications for Photovoltaic Generators," *Engineering, Technology & Applied Science Research*, vol. 9, no. 4, pp. 4371–4376, Aug. 2019, https://doi.org/10.48084/etasr.2829.

[17] M. Y. Allani, D. Mezghani, F. Tadeo, and A. Mami, "FPGA Implementation of a Robust MPPT of a Photovoltaic System Using a Fuzzy Logic Controller Based on Incremental and Conductance Algorithm," *Engineering, Technology & Applied Science Research*, vol. 9, no. 4, pp. 4322–4328, Aug. 2019, https://doi.org/10.48084/etasr.2771.

[18] D. Mezghanni, R. Andoulsi, A. Mami, and G. Dauphin-Tanguy, "Bond graph modelling of a photovoltaic system feeding an induction motor-pump," *Simulation Modelling Practice and Theory*, vol. 15, no. 10, pp. 1224–1238, Nov. 2007, https://doi.org/10.1016/j.simpat.2007.08.003.

[19] Z. Massaq, G. Chbirik, A. Abounada, A. Brahmi, and M. Ramzi, "Control of Photovoltaic Water Pumping System Employing Non-Linear Predictive Control and Fuzzy Logic Control," *International Review on Modelling and Simulations (IREMOS)*, vol. 13, no. 6, pp. 373–382, Dec. 2020, https://doi.org/10.15866/iremos.v13i6.18615.

[20] S. D. Al-Majidi, M. F. Abbod, and H. S. Al-Raweshidy, "A novel maximum power point tracking technique based on fuzzy logic for photovoltaic systems," *International Journal of Hydrogen Energy*, vol. 43, no. 31, pp. 14158–14171, Aug. 2018, https://doi.org/10.1016/j.ijhydene.2018.06.002.

[21] M. H. Sellami, A. Hassen, and M. S. Sifaoui, "Modelling of UV radiation field inside a photoreactor designed for wastewater disinfection Experimental validation," *Journal of Quantitative Spectroscopy and Radiative Transfer*, vol. 78, no. 3, pp. 269–287, May 2003, https://doi.org/10.1016/S0022-4073(02)00216-9.

[22] P. R. Herrick, "Mathematical Models for High-Intensity Discharge Lamps," *IEEE Transactions on Industry Applications*, vol. IA-16, no. 5, pp. 648–654, Sep. 1980, https://doi.org/10.1109/TIA.1980.4503847.

[23] K. Ouelhazi, A. Ben Chaabene, A. Sellami, and A. Hassen, "Multivariable model of an ultraviolet water disinfection system," *Desalination and Water Treatment*, vol. 67, pp. 89–96, 2017.